Petter Nicolai Krohg

Wind field measurements in urban environments

Master's thesis in Sustainable Energy
Supervisor: Tania Bracchi
June 2021

Master's thesis

NTNU
Norwegian University of Science and Technology
Faculty of Engineering

NTNU
Kunnskap for en bedre verden

Petter Nicolai Krohg

Wind field measurements in urban environments

Master's thesis in Sustainable Energy
Supervisor: Tania Bracchi
June 2021

Norwegian University of Science and Technology
Faculty of Engineering

NTNU
Norwegian University of
Science and Technology

Preface

This master thesis has been conducted as a part of the Master's program in Sustainable Energy at the Faculty of Engineering - Energy and Process Engineering at the Norwegian University of Science and Technology - NTNU in the spring of 2021. The study was a continuation of my project thesis completed in the fall of 2020, The master thesis was performed with the purpose of evaluation the wind conditions on a roof in an urban environment, and comparing the results to standards for wind turbines in rural environments. The problem description is stated below.

Problem Description: As the worlds population continues to rise, the topic regarding urban wind is more relevant than ever before. Energy production in urban environments will help reduce transmission losses which in turn will help lower emissions and increase efficiency. Wind maps are available for open fields but not for urban environments. Due to the buildings and constructions the airflow is complex and not fully understood. This project aims to measure the wind field around a building at the NTNU campus Gløshaugen located in Trondheim. The measured data will be analyzed in terms of wind velocity and turbulence intensity and evaluated with the standard IEC6400-2 which is used to evaluate wind fields for small wind turbines in open and flat environments.

I would like to express my gratitude to Tania Bracchi for the opportunity to work with an exiting topic, as well as the guidance, help and encouragement throughout this thesis. I would also want to show my appreciation for the support and help from Yannick Jooss. Lastly i would like to thank my cohabitant, Hanna Lillehaug for the support throughout the project.

Trondheim, 11th June 2021

Petter Nicolai Krohg

Abstract

In the quest of lowering global and local emissions, the topic of urban wind is increasingly more popular. The operating conditions for a Small Wind Turbine (SWT) in an urban environment are harsh due to the complex wind flow and increased turbulence intensity levels caused by buildings and structures. In order to operate a wind turbine safely and reliably, the turbulence intensity at the specific site must be evaluated.

As a part of an ongoing campaign at Norwegian University of Science and Technology (NTNU), this study aims to measure and analyze the wind conditions on top of a building located at NTNU campus Gløshaugen in the city center of Trondheim. The measured values for wind speed and direction were performed using an ultrasonic 3D anemometer located on the top of one of the two tallest building at campus Gløshaugen. To evaluate the wind conditions the The International Electrotechnical Commission standard (IEC) standards IEC61400-1 and IEC61400-2 were used. As defined in the standards, the standard deviation of the horizontal wind speed was calculated for 10-minute intervals, and then used to calculate the turbulence intensity for every interval. In addition to the IEC standards evaluation, the turbulence intensity was calculated in sections of 30° as stated in Measnet standard for evaluating site specific wind conditions to get a better understanding of how the surroundings affect the wind flow in terms of turbulence intensity and wind speed. Since the IEC standards evaluate the wind profiles in open rural areas, with a more uniform boundary layer the varying wind direction in an urban environment was evaluated using 1-minute intervals. Lastly, the vertical wind speed was analyzed to determine the impact of nearby buildings and obstructions present on the roof.

The comparison between the IEC standards and the calculated turbulence intensity at the site reviled that the standards underestimate the turbulence intensity in an urban environment, and is not suitable to evaluate sites with complex wind profiles. The turbulence intensity levels in the 30° sections showed that the wind speeds were increasing as they approached the South wall of the central building. When these sections were compared to the vertical wind speed in the same sections, the results showed that the anemometer is located in the acceleration zone when the wind flow encounters the South wall. The results regarding directional changes in the 1-minute intervals showed an average directional change of 26° from one minute to the next. This implies that a Vertical Axis Wind Tur-

bine (VAWT) could be more suitable due to the rapidly changing wind direction on the roof. The influence from the other tall building on campus did not impact the results for vertical wind speed, Which was expected due to the short distance between them.

Sammendrag

Ettersom verden streber etter å senke klima utslipp og forurensing blir fokuset mer og mer rettet mot fornybar energiproduksjon. Kan vind produksjon i urbane miljøer bidra til å senke både lokale og globale utslipp. Et problem med dette konseptet er at bygninger, og andre strukturer forstyrrer den naturlige vindstrømmen og forårsaker en rekke fenomener som gjør forholdene til en vindmølle krevende. Som en del av et større forskningsprosjekt på NTNU, skal denne studien evaluere vindforhold i et urbant strøk. Hensikten med denne oppgaven er å kartlegge vindforholdene på et tak på en bygning i et urbant miljø for å øke forståelsen om hvordan vindstrømmen bil påvirket av de ytre faktorer. NTNU campus Gløshaugen ligger i Trondheim by, plassert på en høyde med bakker rundt hele området. Målingene skal utføres med et 3D ultrasonisk anemometer som måler vind hastighet, vind retning og temperatur. Disse parameterne skal brukes for å evaluere turbulens nivået, på ett av de to høyeste bygningene på Gløshaugen. Resultatene ble sammenliknet med to IEC standarder, og viste at disse standardene undervurderer turbulenser nivået i et urbant strøk. I tillegg til å sammenlikne resultatene med disse standardene, ble turbulens intensiteten delt opp i seksjoner på 30°, og viste at vind hastighetene økte når vinden blåste direkte på sørveggen av bygningen. Disse resultatene førte til en evaluering av den vertikale vind hastigheten som viste at anemometeret var plassert i akselerasjons sonen ved sørlige vind retninger. Det ble også avdekket at vindretningen endrer seg i snitt 26° hvert minutt, noe som er ekstremt høyt sammenliknet med andre resultater fra andre rapporter. Siden vindhastigheten endrer seg så drastisk hvert minutt, er det sannsynlig at en vertikal akslet vind mølle passer bedre i dette tilfellet. Det ble også undersøkt hvordan den like høye bygningen rundt 50 meter nord for det aktuelle taket ville påvirke vindstrømmen uten at dette førte til noen spesielle funn.

Contents

Figures

Tables

Acronyms

CFL Constant Flux Layer.

HAWT Horizontal Axis Wind Turbine.

IEC The International Electrotechnical Commission standard.

ISL Inertial Sublayer.

ML Mixed Layer.

NTM Normal Turbulence Model.

NTNU Norwegian University of Science and Technology.

NWP Normal Wind Profile.

RSL Roughness Sublayer.

SWT Small Wind Turbine.

UBL Urban Boundary Layer.

UCL Urban Canopy Layer.

USL Urban Surface Layer.

VAWT Vertical Axis Wind Turbine.

Chapter 1

Introduction

As the total energy demand in the world is constantly increasing and the goals of lower emissions are focused, wind power is steadily increasing in popularity. 2019 was a good year for wind energy, with a global increase of onshore wind installations of 17%. As an initiative to increase the share of renewable energy even further, Norway and other countries aim to move to a subsidy-free deployment of wind farm after 2021. Norway increased the total installed capacity by $785MW$ in 2019, which is an increase of 45% yielding a total installed capacity of $2.4GW$[1]. The majority of the global installed capacity originates from larger wind farms, due to the costs associated with building infrastructure for wind parks are extensive. Since the majority of the wind farms are located in uniform flat environments away from the consumers. Pre-existing infrastructure like transport lines for electricity and roads for transport of the wind turbines and building materials must be built for every project. This makes the construction of large scale wind farms are more cost efficient than small ones.

When potential wind sites are evaluated, the mean wind speed is a very important factor due to the potential output power of a wind turbine is defined using the cube of the wind speed. Since a wind turbine normally is located in open rural areas, the wind speeds are generally higher than in urban environments. The rural areas has less disturbances in forms of objects which can reduce the efficiency and cause increased stress on a wind turbine. The knowledge about the characteristics in the lower part of the atmosphere in rural areas are well documented and known in terms of the boundary layer, wind speeds, and turbulence intensity. When it comes to urban environments the wind flows are more complex due to the number of disturbances caused by buildings, constructions, and vegetation which are not affect the efficiency of a wind turbine. As the demand for more renewable energy increases, the research and interest around SWT in urban environments is increasing. The advantages of producing local wind energy are that the infrastructure required by the large scale wind turbines are not needed. The shorter distance between the consumer and the wind turbine also reduces the transport losses in the power lines, thus increasing the total efficiency. A SWT is normally not designed for highly turbulent wind conditions, but for conditions more similar

to what one could expect in an open rural area. The increased roughness in an urban environment causes more turbulent wind flows, which causes more structural stress on the wind turbine that could cause failure that potentially results in material damage to nearby structures or even injuries to people.

1.1 Background

IEC is a global nonprofit organization that works to underpin infrastructure and international trade of electrical and electronic goods. Their work includes facilitating technical innovations, infrastructure development, sustainable energy access, and more. The organization has over 170 member countries and provides a global standardization platform that is neutral and independent[2].

IEC has a series of standards regarding the evaluation of potential sites for wind farms. Which include the standard *IEC61400-1:Wind energy generation systems - part 1: Design requirements*. The standard classifies three different wind turbine classes depending on the annual wind speeds, with four turbulence intensity levels for every class. The different classes are then compared to the annual wind speed and turbulence intensity measured at the site. When the class is determined, a wind turbine suited to the specific site can then be designed to ensure safe and reliable operation.

The standard *IEC61400-2:Wind turbines - part 2: Small wind turbines* uses the same evaluation method as *IEC61400-1*, and have four different SWT classes using the same turbulence intensity level.

Some issues arise when looking into the standards, as they are not intended to be used for evaluating wind conditions in an urban environment. The topic of urban wind is a new field of interest, with little research on the topic. From an economical view, a large scale wind farm would be more profitable than SWT's, but form an environmental view urban wind is an interesting topic which can contribute to lower local and global emission.

1.2 Objectives

As a part of an ongoing research project around the topic of urban wind, this study will evaluate the measured wind conditions on a roof of a building located on campus Gløshaugen at NTNU.

The main goal of this study is to evaluate the wind condition in an urban environment using an ultrasonic 3D anemometer. These measured results will be compared and evaluated using the IEC wind turbine standards IEC61400-1 and IEC61400-2, to determine if these standards are viable when evaluating wind conditions in the complex urban environment. Parameters such as wind speed, wind direction and turbulence intensity will be evaluated. In addition, the site specific observations will be evaluated in terms of disturbances, flow separation, and fluctuation in wind direction. In context, boundary layer development is presented

together with wind flow around buildings. As well as wind turbines, sonic anemometers, standards, and statistical parameters used in this study will be presented in chapter 2. In chapter 3 site specific details are presented along with the methodology used when evaluating the results. The results are presented and discussed in chapter 4 and lastly the conclusion in chapter 5.

Chapter 2

Theory

This chapter introduces the theory used in this study, as well as mathematical concepts used to evaluate the wind conditions at a potential wind energy site, including standards for evaluating results.

2.1 Meteorlogy

2.1.1 The Planet boundary layer

The earth's troposphere extends from the surface of the earth up to an average altitude of $11km$, but only the lowest $\sim 2km$ are affected by the surface of the earth. The planet boundary layer is often referred to as the Atmospheric Boundary Layer (ABL), can be defined as the part of the troposphere that is directly influenced by the presence of the earth surface and other forces influencing the flow close to the earth. These forces include friction, evaporation and transpiration, heat transfer, pollution emissions and terrain that influences the wind flow. Figure 2.1 shows the earth's troposphere where the planet boundary layer is closest to the earth[3].

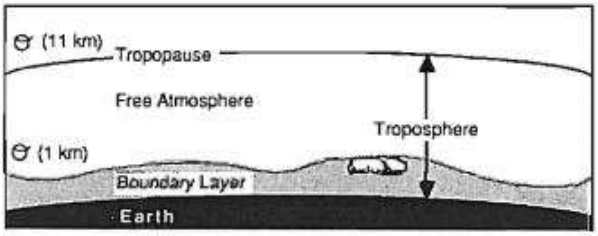

Figure 2.1: The earth's troposphere [3]

The atmosphere heats water and the area around equator and forms a low pressure system which causes the warm air to rise up in the atmosphere before migrating towards the poles. As the warmer air moves up in the atmosphere, cooler air replaces the air around equator, causing a high pressure system and air to blow

across the surface of the earth. Air normally moves from a high pressure area to a low pressure area causing wind[4].

When the air travels along the surface of the of the earth, the friction on the surface affects the wind profile up to 500 meters, depending on the magnitude of the surface friction. The effect is largest close to the surface of the earth, and decreases with the increasing altitude. Figure 2.2 shows how friction affects the wind flow over a flat surface with grass and shown the velocity increase as the altitude increases[5].

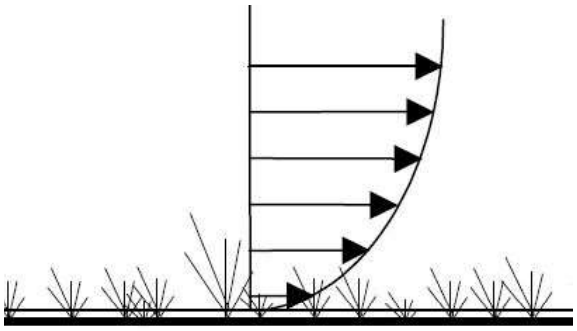

Figure 2.2: Boundary layer development over grass [6]

As a flow encounters buildings and other obstacles, the surface roughness changes which in turn causes the wind flow to tumble and swirl causing turbulence. In addition, rapid changes in wind velocity may occur downwind of the buildings[6]. Figure 2.3 shows a wind flow as it enters a city. This induces a step in the roughness and forms a new Urban Boundary Layer (UBL). The UBL is divides in to several sublayers. Urban Surface Layer (USL) consists of two subsub layers Mixed Layer (ML) and Constant Flux Layer (CFL) or Inertial Sublayer (ISL). The two layers closest to the surface of the earth are the Roughness Sublayer (RSL) and the Urban Canopy Layer (UCL). The RSL is defined as the layer between the rooftops of the buildings and the bottom of the CFL, and the UCL is the layer between the ground and the roof tops of the buildings[7]. Wind flows inside the RSL and UCL are highly turbulent which can be detrimental for a wind turbine, as the turbulence causes vibrations and uneven forces on a wind turbine, which increases the stress on the turbine and reduces the efficiency[6].

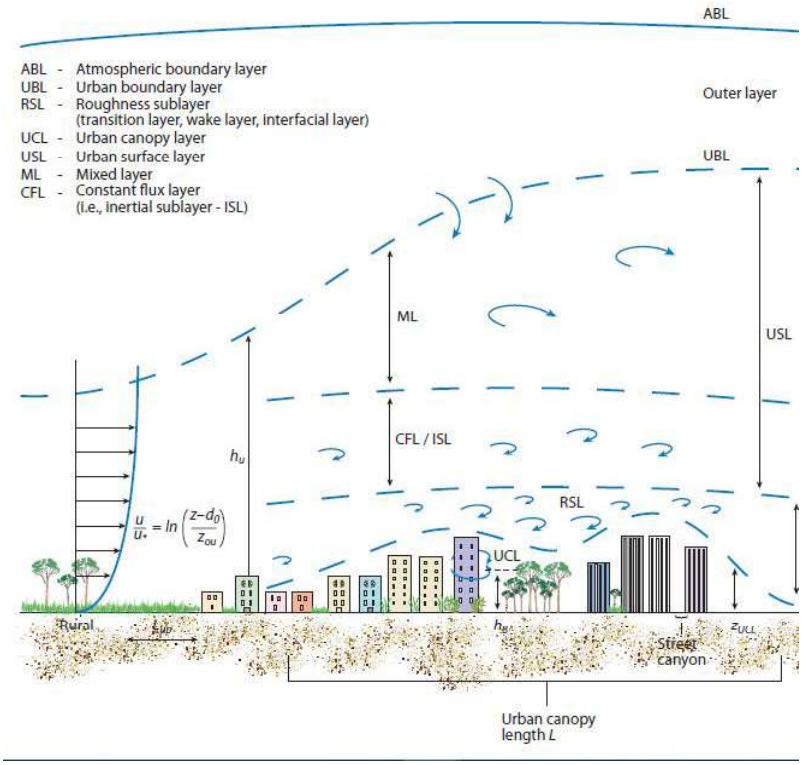

Figure 2.3: Development of the UBL [7]

In addition to the buildings and structures, the topography of the ground greatly affects the wind flow. This causes fluctuations in wind speeds and increases the turbulence intensity causing the operating conditions for a wind turbine to be structurally demanding [8].

2.1.2 Wind flow characteristics in urban environments

When a wind flow encounters a vertical wall it divides into different flows, which occurs around the stagnation point marked with H_s in figure 2.4. The figure shows the flow dividing to the left and right side of a building from a top view (left in the figure). The flow also divides upwards and downwards on the facade from a side view (right in the figure). The pressure is largest at the stagnation point, and determines how the flow develops around the building[6].

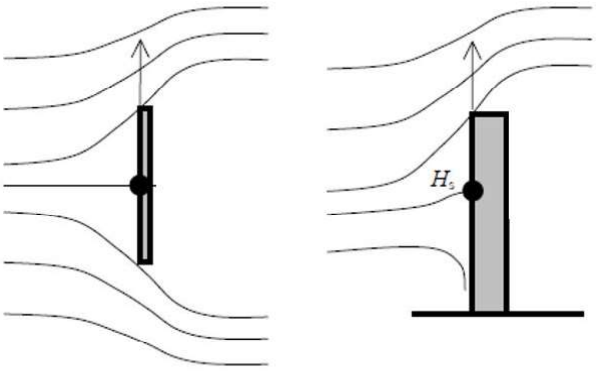

Figure 2.4: Wind flow around building []

As the upwind flow encounters the sharp edges of the roof and sides of the building, the boundary layer separates from the building. The result of this is regions with low velocity with a high level of turbulence. Simultaneously a recirculation zone forms on the roof and sides of the building. Figure 2.5 shows a two dimensional Computational Fluid Dynamics (CFD) simulation of a building with sharp edges on the roof. The figure shows how the separation causes a recirculation zone to form over the roof, determined with the low velocity vectors originating from the downwind side of the building[6].

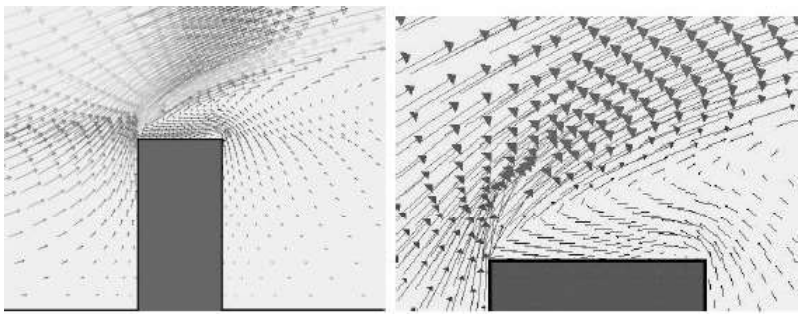

Figure 2.5: Flow separation on building roof [6]

A report from *(Mertens, 2006)*[6] discusses how the separation on the edge of the roof affects the flow and wind speed in the area above the roof. When the separation occurs an acceleration zone will be formed, where the wind speeds are increased. Despite that, an urban wind environment generates harsher working conditions for wind turbines, with generally lower wind speeds and higher turbulence intensities compared to than in open fields. The local phenomenon of the acceleration zone can increase the wind speeds with up to 20% of the undisturbed wind speed upstream. These observations have been noticed above the recirculation zone, as shown in figure 2.5 the wind speed vectors increase above the left edge of the roof.

If evaluating a specific point on the edge of the roof, for example, the left edge in figure 2.5. The report states that the maximum acceleration is found at the upwind side of the building when the wind direction is perpendicular to the specific point. If the wind direction is shifted 180°, thus being perpendicular to the right side of the building, the acceleration zone will be formed on the right edge of the building. And due to the specific point being on the left edge, the point is now inside the recirculation zone. The difference in size of the wind speed vectors on the left vs right sides of the building roof illustrates the phenomenon. The report evaluates three positions on a roof in 3D. The corner of the roof, the center of the roof and on the edge of one of the facades. When comparing the effects in terms of wind speed, the central position gives the overall best wind conditions, and the highest wind speeds are found in the corner on the roof[6].

Other CFD simulations from the report show that the recirculation zones are smaller at the corners of the roof, shown in figure 2.6. As the three dimensional flow separates on the roof and sides of a building, recirculation zones on the roof and sides are formed as well as vortices downwind of the building sides[6].

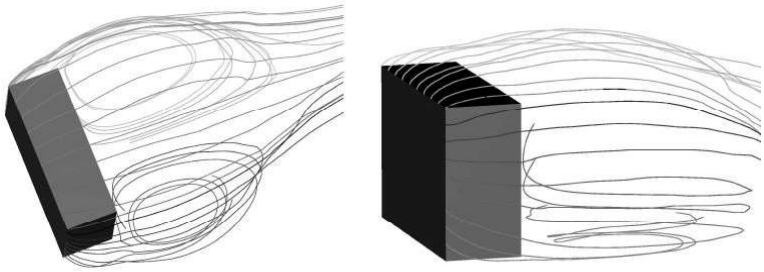

Figure 2.6: Flow separation on three dimensional building [6]

The report *Turbulent Flow Around Two Interfering Surface-Mounted Cubic Obstacles in Tandem Arrangement(Martinuzzi,2000)*[9] evaluates how one cube affects the wind conditions on another cube downwind of the first. As a wind flow encounters the first cube, the flow separation causes an acceleration zone as well as a recirculation zone as described earlier. The study uses two symmetrical cubes with height H and distance between the cubes S. Figure 2.7 shows a vector representation of how the flow develops from one cube to the other when the distance between them increases. Figure 2.7 (a) shows the distance to height factor $S/H = 1$, where the distance is the same as the height. In figure 2.7 (b) the distance to height factor is $S/H = 2$, and $S/H = 4$ in figure 2.7 (c)[9].

When the distance between the two cubes is the same as the height of the cubes, the second cube is highly affected by the separation caused by the first cube. The velocity on the top of the second cube is severely decreased, most likely due to the flow impinging on the top and front of the second cube. The result of this is strong downwards winds and a larger recirculation vortex between the cubes than the other scenarios. The results in (b) show a weaker recirculation vortex between the two cubes, but the size is much larger. Due to the longer distance to

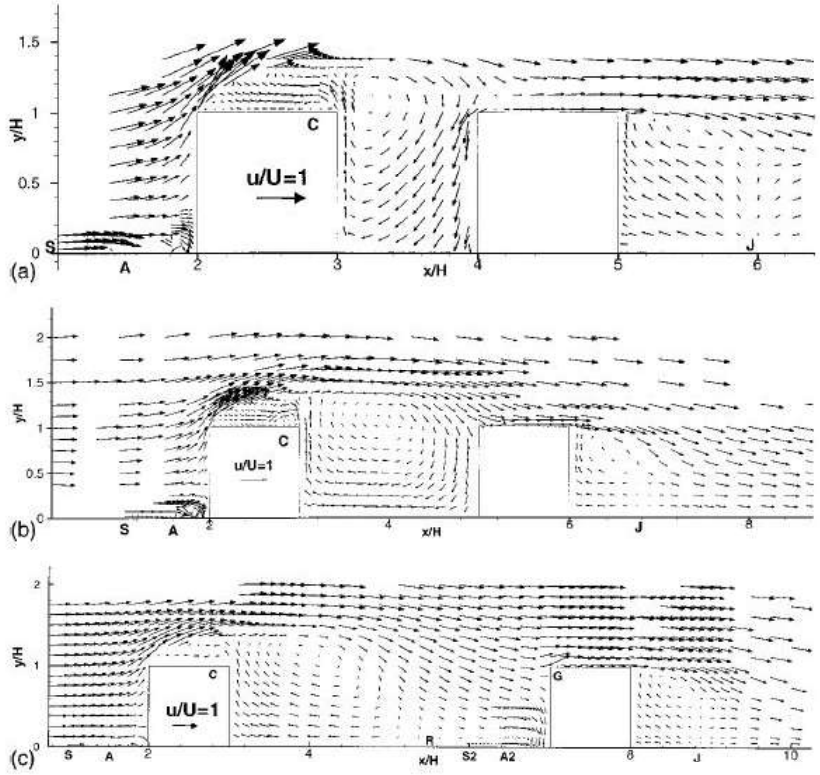

Figure 2.7: Influence of separation for two cubes in series [9]

the first cube, the angle at which the flow encounters the second cube is not as drastic. This causes more of the flow to have less impingement on the face of the cube, but it still takes place on the top of the cube. This causes high turbulence levels and complex flows. The last scenario (c) is least affected by the separation on the first cube and is the only case where there is a small upwards flow at the leading edge of the second cube.

2.2 Wind turbines

Traditional large scale wind turbines are usually located together and make up a wind farm. Such farms can be located either onshore or offshore, and are often placed far away from the consumer. The surroundings are normally flat rural areas, where the wind speeds are considerably higher than in an urban environment. But in some places in cities, the wind speed can reach higher wind speeds. For example, two buildings can create a venturi effect increasing the wind speeds, and separation on sharp edges can create increased wind speeds. There are several downsides of having the wind farms far away from the consumer, one of them is that the long distance transport of the energy induces losses, and thereby

lowering the efficiency. From an environmental view, the large scale wind parks require massive infrastructure which is energy demanding, thus contributing to more emissions. The transport of all materials and equipment to the site also contributes to raising the emissions in the construction phase.

The two main types of wind turbines are the horizontal axis wind turbine HAWT and the vertical axis wind turbine VAWT. A HAWT is defined as a wind turbine where the rotating axle connecting to the generator is horizontal, as shown in figure 2.8 (a) to the left. A VAWT has the rotating axle which connected between the rotor and generator vertically. Figure 2.8 (b) shows a VAWT. The two different types of wind turbines have pros and cons. While the HAWT generally has higher efficiency, they also have more moving parts which result in potentially more failures. The HAWT should always be facing perpendicular to the wind direction, while the VAWT has a uniform design, thus always has the same angle towards the wind[6].

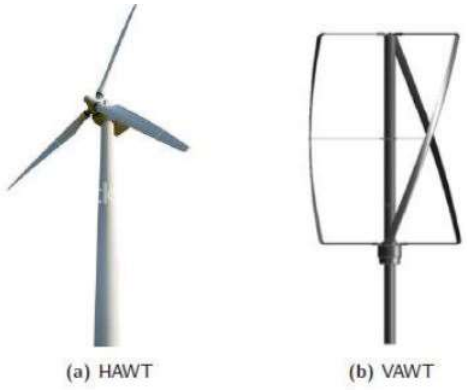

Figure 2.8: HAWT and VAWT

Wind speed is the most important factor for producing electric power from wind energy. The output of a wind turbine is defined in equation 2.1.

$$P = \frac{1}{2} \cdot \rho \cdot A \cdot U^3 \cdot c_p \tag{2.1}$$

The equation shows that the main contributor to the output power of the wind turbine is the cube of the horizontal wind speed U. ρ is the air density and A is the swept area of the wind turbine. c_p is the power coefficient of the wind turbine, which is defined as the electrical output power of the wind turbine, divided by the available wind power at the rotor. In other words, the efficiency of the entire wind turbine[6].

2.3 Sonic anemometers

A sonic anemometer measures the time an ultrasonic pulse uses from one transducer to another and then calculates the wind speed. This type of anemometer

is different compared to traditional measuring instruments like the cup anemometer, due to the lack of moving parts which makes it more reliable and more precise. The sonic anemometers can be configured in two or three dimensions, with up to four or eight transducers. Figure 2.9 show the principle of operation of a sonic anemometer. The Gill windmaster 3D sonic anemometer uses six transducers, three upper and three lower transducers. The upper transducer sends a signal to its opposite lower transducer, at the same time the receiving lower transducer sends another signal to the opposite transducer. This happens for all three pairs of transducers[10].

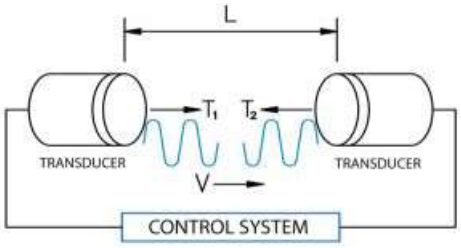

Figure 2.9: Principle of operation [10]

This type of anemometer is independent of factors like temperature and rain. The Gill instruments WindMaster has two different output formats are available for configuration. Either the polar definition with one wind speed in the horizontal (U-V) plane and the vertical wind speed W, with a direction range of $0-359°$ in reference to the north spar. Or decomposed into U, V, and W where $+U$ is defined as the wind speed component aligned with the north spar marked on the base of the anemometer. $+V$ is defined as the counterclockwise 90° from the north spar. $+W$ is defined as the vertical wind speed component as shown in figure 2.10. The figure also shows the transducers marked with 1, 2 and 3. [10]

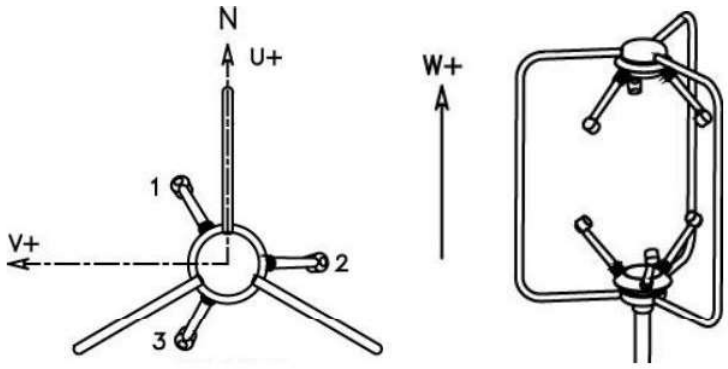

Figure 2.10: U,V and W alignment [10]

2.4 Statistical parameters

This section will introduce statistical parameters used in this report.

2.4.1 Mean values

The mean value is the average value over a set of data. Equation 2.2 shows the definition of the mean value.

$$\mu = \frac{1}{N}\sum_{i=1}^{N} A_i \tag{2.2}$$

Description:

μ The mean value

N is the number of observations in the data set

A_i is the specific value in row i

2.4.2 Standard deviation

Standard deviation is a statistical parameter that describes the amount of variance in a set of values compared to the mean. When the standard deviation is low the values tend to lie close to the mean, if the standard deviation is high the values tend to be far from the mean. The standard deviation is defined as the square root of the variance and is shown in equation 2.3 where A is a vector with N observations.

$$\sigma = \sqrt{\frac{1}{N-1}\sum_{i=1}^{N}(A_i - \overline{A})^2} \tag{2.3}$$

Description:

σ Standard deviation

N is the number of observations in the data set

A_i is the specific value in row i

$\overline{A}$ is the mean of all values in vector A

2.4.3 Skewness and Kurtosis

In addition to standard deviation skewness and kurtosis contributes to describe the distribution. Skewness is a measure of asymmetry around the mean for a given distribution. The skewness can either be neutral, positive, negative, or undefined and describes which way the tail of the distribution is trending. If positive, the "tail" is trending to the right, if negative the trend is to the left. If the $skewness = 0$, the $mean = median$ and the distribution is symmetric. Skewness is calculated as shown in equation 2.4.

$$s = \frac{E(U-\mu)^3}{\sigma^3} \tag{2.4}$$

Description:

s Skewness

σ Standard deviation of U

μ is the mean of U

U is the wind speed

$E(t)$ is represents the expected value of the quantity t

Skewness and the standard deviation alone do not fully describe the distribution, since two different distributions can be symmetrical with $skewness = 0$, and have the same standard deviation and still not be identical. Kurtosis is a measure that describes the shape of the distribution in terms of how the peaked it is. A normal distribution has a $kurtosis = 3$, which is called mesokurtic, if the kurtosis is lower than 3, the distribution has thicker "tails" and the peak is lower compared to the normal distribution. If the kurtosis is higher than 3 the peak is higher than the normal distribution and has thinner "tails", this distribution is called leptokurtic. Equation 2.5 shows the definition of kurtosis.

$$k = \frac{E(U-\mu)^4}{\sigma^4} \tag{2.5}$$

Description:

k Kurtosis

σ Standard deviation of U

μ is the mean of U

U is the wind speed

$E(t)$ is represents the expected value of the quantity t

2.4.4 Turbulence intensity

Turbulence intensity is defined as the standard deviation of the horizontal wind speed over a period of 10 minutes, divided by the mean wind speed for the same time interval. This gives a measure of how much the wind speed fluctuates compared to the mean. Equation 2.6 shows the definition of turbulence intensity used in this study.

$$I = \frac{\sigma}{U} \tag{2.6}$$

Where I is the turbulence intensity, σ is the standard deviation of the horizontal wind speed in the 10-minute interval and U is the mean wind speed over the same 10-minute interval.

2.5 IEC standard IEC61400-2

The International Electrotechnical Commission IEC standard IEC61400-2 provides guidance when designing a SWT, which is defined as a wind turbine with a swept area of less than $200m^2$. The standard specifies requirements that need to be fulfilled in order to ensure that the wind turbine is able to withstand the external loads that is affected by the varying wind conditions, including turbulence intensity. Defining a required level of safety and quality will in turn achieve operational durability and reliability. The standard is divided into four groups of SWT classes (I-IV) and describes the different wind conditions for different types of sites. The different classes give information about the reference wind speed, annual average wind speed, and turbulence intensity. Table 2.1 shows the information for the different SWT classes. The external conditions mainly refer to wind conditions which are divided into two subgroups, normal wind conditions, and extreme wind conditions[11].

Table 2.1: Design parameters for IEC61400-2

SWT Class	I	II	III	IV	S
$U_{ave}[m/s]$	10	8.5	7.5	6	*
$I_{15}[-]$	0.18	0.18	0.18	0.18	*
$a[-]$	2	2	2	2	*

Description:

* Values specified by the designer

U_{ave} Annual average wind speed measured at hub-height

I_{15} Dimensionless characteristic value of turbulence intensity at 15 m/s at hub-height

a Dimensionless slope parameter used to calculate the standard deviation for calculating turbulence intensity

2.5.1 Normal Wind conditions

Normal wind conditions is defined as the frequently occurring conditions when normally operating a SWT. The classifications of the different turbine classes $(I - IV)$ assume Rayleigh distributed wind. The distribution of the wind speed at the site is important when calculating the specific loads because it determines the frequency of the different load conditions. Equation 2.7 determines the cumulative probability that the wind speed is lower than a given wind speed.

$$P_{Rayligh}(U_{hub}) = 1 - e^{-\pi\left(\frac{U_{hub}}{2U_{ave}}\right)^2} \tag{2.7}$$

U_{hub} is the mean wind speed measured at hub height for a 10 min interval and U_{ave} is the annual wind speed mean. The Normal Wind Profile Normal Wind Profile (NWP) determines the variation of the vertical wind speed and is calculated with equation 2.8. The assumed wind profile is used to define the average vertical wind shear across the swept area of the wind turbine.

$$V(z) = U_{hub}\left(\frac{z}{z_{hub}}\right)^{\alpha} \tag{2.8}$$

Where z is the height above the ground, z_{hub} is the hub-height and α is a power of law exponent which shall be assumed to be 0.2.

The standard uses the Normal Turbulence Model Normal Turbulence Model (NTM) to describe the turbulence intensity and include the influences of fluctuation in wind direction and speed. The model determines the standard deviation of the horizontal wind speed σ_1 as shown in equation 2.9.

$$\sigma_1 = I_{15}\frac{(15 + aU_{hub})}{a + 1} + \Delta\sigma_1 \tag{2.9}$$

Where I_{15}, a is given in table 2.1 and $U_{hub)}$ is the measured wind velocity mean at hub height over a time span of 10 minutes in three dimensions. $\Delta\sigma_1$ is a modification to the equation which allows the model to work with different percentiles which are shown in equation 2.10.

$$\Delta\sigma_1 = 2(x - 1)I_{15} \tag{2.10}$$

Where x is determined from the normal distribution function, for example the 95$^{\text{th}}$ percentile. The turbulence intensity is then defined as stated in equation 2.6 where $\sigma = \sigma_1$ and $U = U_{hub}$. The results will show the expected turbulence intensity for the 10 minute interval as stated by IEC[11].

Extreme wind conditions are also considered in this standard, but are not considered in this study as the total duration of the measurements is less than 5 months.

2.6 IEC standard IEC61400-1

Compared to the IEC standard 61400-2 introduced in section 2.5, the standard IEC61400-1 can be applied to wind turbines of all sizes, thus can be used to evaluate small wind turbines. The scope of the standard includes specific and essential design parameters to ensure safe operation in terms of structural integrity or damage which can occur throughout the lifetime of the wind turbine. The standard also considered all subsystems, internal electrical systems, mechanical systems, and support structures. The different turbulence categories A+, A, B, C are designed to cover the majority of sites, but due to the diverse wind conditions of different sites, the results may not be as precise a representation of every site. Table 2.2 shows the design parameters defined in the standard[12].

Table 2.2: Design parameters for IEC61400-1

Wind Turbine Class	I	II	III	S
$U_{ave}[m/s]$	10	8.5	7.5	*
$I_{ref,A+}[-]$	0.18	0.18	0.18	*
$I_{ref,A}[-]$	0.16	0.16	0.16	*
$I_{ref,B}[-]$	0.14	0.14	0.14	*
$I_{ref,C}[-]$	0.12	0.12	0.12	*

Description:

All values apply at hub height

* Values specified by the designer

U_{ave} Annual average wind speed

$I_{ref,A+,A,B,C}$ Dimensionless characteristic value of turbulence intensity for very high, high, medium, and low turbulence characteristics respectively

2.6.1 Normal wind conditions

Similar to the standard IEC61400-2, this standard uses the same wind speed distribution and NWP defined in equations 2.7 & 2.8 respectably, as described in section 2.5. This standard also uses the NTM, but the standard deviation is defined differently from IEC61400-2. Equation 2.11 shows the standard deviation defined in this standard.

$$\sigma_2 = I_{ref} \cdot (0.75 \cdot U_{hub} + b) \tag{2.11}$$

Where $b = 5.6m/s$. σ_2 is the representative value of the standard deviation of the 90% quantile of the wind speed measured at the hub height. U_{hub} is the 10

minute mean of the wind speed measured at hub height. The value I_{ref} is chosen from the different turbulence classes shown in table 2.2.

The turbulence intensity is defined the same as shown in equation 2.6, but using σ_2 instead of σ[12].

The standard also evaluates extreme wind conditions, including extreme changes in wind speed and direction as well as extreme gusts. But these will not be evaluated in this report.

2.7 Measnet - Evaluation of site-specific wind conditions

Measnet is a collaboration of different measurement institutes, tasked to achieve a uniform interpretation of the different standards associated with evaluating wind conditions. The diverse definitions of terms and measuring procedures used to evaluate wind conditions induce problems when comparing results from one site to another. The standard gives advice on what definitions and techniques to use when measuring, evaluating the data when interpreting the site-specific results and how to report the results.

Evaluation of the thermal stability is recommended, but especially at sites where large temperature ranges are expected. The measurements should include at least 12 months of measurements to include all seasons. The recommended configuration is to use two temperature sensors at different heights, where one is located within 10 meters of the anemometer.

When reviewing the data and gaps in the measurements caused by wind speeds being lower than the threshold of the anemometer or corrupt measurements the missing data should be reconstructed with relevant data from other nearby sensors.

Turbulence intensity I should be defined as shown in the IEC standards, using equation 2.6, using the standard deviation of the 10-minute wind speed intervals. Measnet and the IEC standards use horizontal wind speed when evaluation the turbulence intensity.

In addition, the turbulence intensity has to be specified for sections of 30° using wind speed bins of $1m/s$, if a significant number of measurements are available.

The standard also describes how to evaluate other statistical parameters that will not be considered in this report. These include flow inclination of the topological variations around the area of the measurement site. As well as the wind shear exponent which requires wind data for two different heights[13].

Chapter 3

Method

This section describes the method used when evaluating potential locations for placement of the anemometer, and the evaluation of measurements.

3.1 Measuring Instrument

The instrument used to measurements wind speed and direction is the Gill instruments WindMaster 3D ultrasonic anemometer. It has a range of $0-50m/s$ and a resolution of $0.001m/s$. The wind direction is measuring $0-359^{\circ}$ with a resolution of 0.1°. Figure 3.1 shows the anemometer as it arrived from the distributor, without any mounting system or wiring harness, this had to be produced for this project specifically[10].

Figure 3.1: Gill instruments WindMaster [10]

As described in section 2.3, this anemometer uses six transducers to measure the wind speed and velocity. The anemometer also measures temperature with a range of $-40^{\circ}C$ to $+70^{\circ}C$. The output format of the anemometer can be chosen by the user, either polar or U,V,W vector outputs. The sampling frequency can also be determined by the user in a range of $1-20Hz$. The output format of the log file is a text file, where one row represents one sample. If the sampling frequency is

$20Hz$, 1 second is recorded as 20 rows of data. Each column represents one parameter like wind direction, wind speed or temperature. The output format used in this project is polar output, initially with $1Hz$, but this was changed to $20Hz$ 16.04.2021. The data was saved every other hour, due to the low ram capacity of the laptop.

3.2 Preliminary work

3.2.1 Measuring site

NTNU is Norway's largest university with 10 campuses in Trondheim. Campus Gløshaugen is located in the city center of Trondheim in Norway on top of a hill around 42 meters above the sea level. Figure 3.2 shows the Topological map and shows the hills surrounding the campus. The buildings on are varying in size, where central buildings 1 & 2 are the tallest buildings with 13 floors and a height of around 43 meters from the ground. Central building 1 is marked with a yellow star, and central building 2 marked with a red star is located around 56 meters North-West of central building 1. There is a lower building between the two central buildings that connects them together. The height between the roof of this building and the roof of the central buildings is approximately 29 meters. Two identical lower buildings are located on the Northside of central building 2, and South of central building 1. The surrounding area of the campus is mostly parks, but also residential areas.

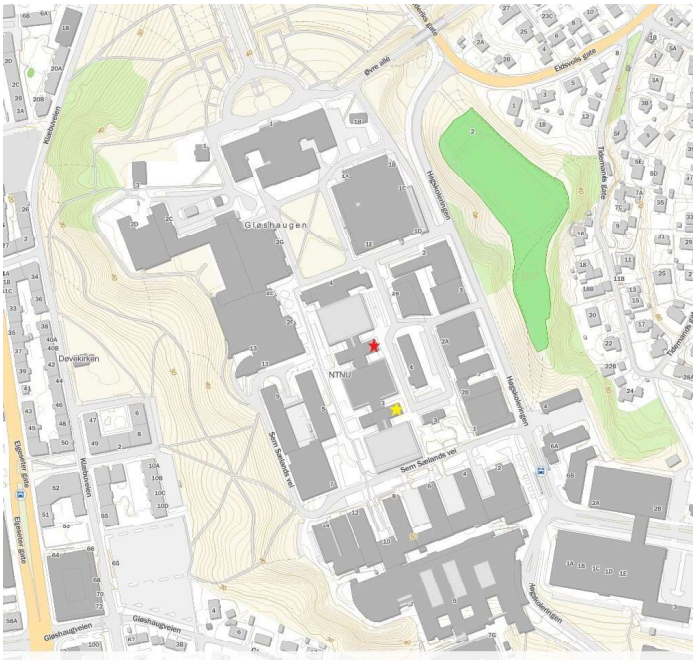

Figure 3.2: Topological map of campus Gløshaugen

Several roofs on the campus were evaluated, but the roof of Central building 1 was chosen as the best candidate based on simulations performed on campus from the report *Urban wind: CFD analysis of Gløshaugen campus based on measured data (Burkelang, 2018)*[14]. And a better candidate than central building 2 due to the main wind direction being from the South. Figure 3.3 shows the simulation results when the wind is approaching the campus from the main direction and shows that the turbulence intensity is lowest on the roof of central building 1 which is marked with a white arrow.

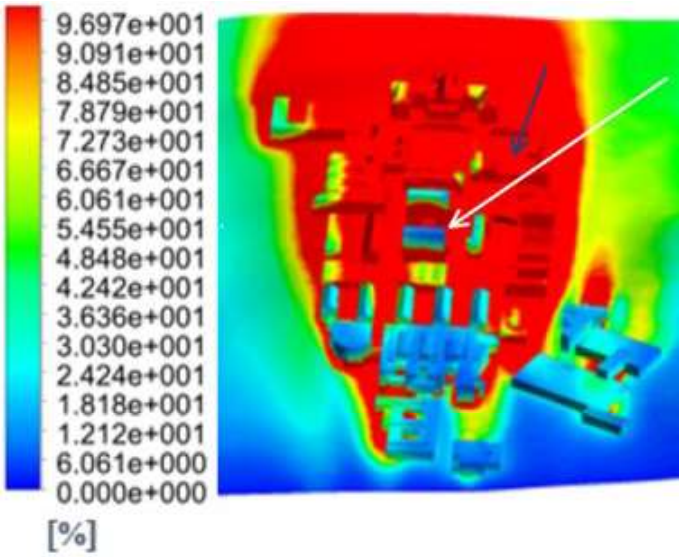

Figure 3.3: Turbulence intensity at campus Gløshaugen [14]

The panoramic photos showed in figure 3.4 where taken on the roof of central building 1, and show the surrounding area as well as the obstructions which are present on the roof. Figure 3.4a shows the view on the roof from the South-West to North-East. It also shows the roof of central building 2, which is located almost in the middle of the photo. The second figure 3.4b shows the view from North-West to South-East, where the roof of the central building 2 is to the left in the photo. The last figure 3.4c shows the view from South-East to South-West.

(a) Panoramic photo showing South-West to North-East

(b) Panoramic photo showing North-West to South-East

(c) Panoramic photo showing South-East to South-West

Figure 3.4: Panoramic photos of the site

The roof of Central building 1 has four solar panels mounted along the south wall of the roof, which are a part of another experiment at NTNU. These solar panels are designed to follow the direction of the sun and can be seen to the right in figure 3.4c. In addition, there are two identical smaller installations on the West and East side of the building which can be seen to the right in figure 3.4a, and to the left in figure 3.4c. The placement of the anemometer in respect to the building edges is 2.5m from the South wall, 6.0m from the East wall, 35.0m from the West wall, and 8.3m from the North wall. And thus placed much closer to the South and East edges, than the North and West edges. When the anemometer was mounted on the roof, the North spar was aligned using a compass to ensure that the anemometer was as close as possible to the North.

Figure 3.5: Map of campus Gløshaugen showing the alignment of the building with center at the anemometer placement

Figure 3.5 shows a map of campus and a compass gauge, showing the angles around the anemometer. The anemometer is placed in the center of the compass. This gives a better overview of the different wind directions and the surroundings, in combination with the panoramic photos in figure 3.4. The different directions will be discussed later in the report, but for future reference, the North wall is defined as the wall that encounters wind for directions between $260° \sim 0°$, and the South wall encounters wind from directions $120 \sim 230°$.

3.2.2 Designing mount and wiring harness

The anemometer did not arrive with any forms of mounting, this was designed for this specific project. When evaluating different positions on the roof of Central building 1 it was decided to share a mount with some existing equipment mounted on the roof to reduce the number of holes in the roof. After several revisions of the design, a final version was concluded, and produced in house at NTNU. Figure 3.6 shows the mast designed, and the shared mount in the roof. The mast is designed to be adjustable where the height can be adjusted from $2.3m$ to $3.6m$ measuring from the bottom of the roof to the top of the anemometer.

Figure 3.6: Final version of mast

After the design of the mast was finished the wiring loom for the anemometer was produced following the manufacturer's specification. The wiring harness consists of a $5m$ long RS-232 data cable with a RS-232 USB adapter, as well as an external $12V$ external power supply, where both merged into the same connector at the base of the anemometer. As the maximum length of the data cable is limited to $6.5m$ by the manufacturer the laptop used to datalog the measurements had to be mounted outdoors. A weatherproof Zarges transport box with waterproof cable guides was used to provide a safe and dry environment for the laptop. Figure 3.7 shows the anemometer mounted on the roof together with the box with electronics.

Figure 3.7: Anemometer mounted on the roof

3.3 Analyzing results

All the calculations, plotting, and sorting of data in this project was performed using MATLAB. The scrips used were made by me, specific for this project.

3.3.1 Importing and modifying data

Some of the data will be logged as an error. This can happen if for example, the wind speed is lower than $0.05 m/s$, the anemometer will not log the data. This creates gaps in the data set, and when imported to MATLAB, the value shows up as NaN. Since this project only uses one anemometer, the data cannot be reconstructed as stated in the Measnet standard using the available data from nearby anemometers. Instead, a script was made to replace all NaN values with zeros, then a for loop which replaces the zeros with the previous value, if larger than 0.05. This way, the last known recorded wind speed, direction and temperature were used where the data was missing.

3.3.2 Wind speed and direction mean values

The wind direction logged by the anemometer has a range of $0 - 359°$, where $0° = North$, $90° = South$, $180° = South$ and $270° = West$. When calculating the 10 minute mean of direction, the data was sorted in columns of 12000 values which represents 10 minutes of data with a sampling frequency of $20 Hz$. Then the mean of every column was calculated, yielding the mean wind direction for every 10-minute interval. The wind speed was sorted and calculated in the same manner, before the data was merged into one matrix.

3.3.3 Standard deviation

The standard deviation of the wind speed describes the spread of the data compared to the mean and was calculated according to equation 2.3, as described in section 2.4.2. Since the turbulence intensity is calculated for every 10 minutes, the standard deviation was calculated from the matrix after sorting the wind speeds in 10-minute columns as described in section 3.3.2 yielding the standard deviation for every interval. With the standard deviation, the turbulence intensity can now be calculated.

3.3.4 Turbulence intensity

The turbulence intensity was calculated using the equation 2.6, as stated in the Measnet standard. Using the standard deviation of the horizontal wind speed to calculate the turbulence intensity for every 10-minute interval. Then the turbulence intensity and standard deviation were merged into the same matrix as the mean wind direction and speed.

3.3.5 Skewness and Kurtosis

The skewness and kurtosis was calculated as stated in section 2.4.3, using the MATLAB functions $y = skewness(X)$ and $k = kurtosis(X)$. Together with the standard deviation, the skewness describes how asymmetrical the distribution is. If the skewness is equal to zero, the distribution is symmetrical. If positive, the "tail" of the data will trend to the right, and to the left if negative compared to the mean value. Similar to skewness, kurtosis is a measure that also describes the shape of the distribution, but in terms of the tails of the data. If for example the majority of the data is spread around the mean, this implies that the shape of the distribution is more pointy than a normal distribution, thus the "tails" are shorter.

3.3.6 Section analysis of wind data

The Measnet guidance recommends specifying the turbulence intensity in sections of 30° using $1m/s$ bins and calculating the turbulence intensity as stated in the IEC standard IEC61400-1 if a significant number of underlying measurement values are available. But neither Measnet nor the IEC standards define how the sorting of the data should be done. The two logical solutions would be to either sort the data by direction first, then sort the wind speeds into $1m/s$ bins. And lastly calculating the turbulence intensity in the 10-minute intervals as stated in the Measnet guidance, and defined in IEC61400-1. The other option would be to calculate the 10-minute intervals first, then use the mean direction and wind speed to sort the data into the directional sections and wind speed bins of $1m/s$.

3.3.7 Change in wind direction

When measuring the wind speed on a roof there are a lot of factors that can affect the flow. As described in section 2.1.2 the wind flow in urban environments is highly affected by the surrounding buildings, which can affect the wind direction. When evaluating directional change the data set should be divided into smaller intervals than the turbulence intensity. Intervals of $\tau = 1$ minute were therefore used to evaluate the directional change. After sorting all measurements into bins of 1200 observations, representing $\tau_F = 1$ minute, the mean of each interval was calculated. To determine the directional change between two adjacent intervals they were subtracted to each other as shown in equation 3.1.

$$\delta_t = \theta_{\tau_i} - \theta_{\tau_{i+1}} \tag{3.1}$$

Where δ_t is the difference in angle and θ is the wind direction mean over the 1-minute interval i. The calculation of δ only gives the difference in terms of values, and not the actual difference in angle. For example the angle of interval 1 could be $\theta_{\tau_1} = 350°$ and angle of interval 2 could be $\theta_{\tau_2} = 10°$ the calculation would show a difference of 340°, where in reality the angle between the two intervals is 20°. To resolve this problem every value of δ_t over 180° was subtracted by 360°, and added to every value of δ_t below −180°, resulting is a range of −180° to 180°.

This will give a correct representation of the distribution of the change in wind direction, but in the case of the example, the directional change will be $-20°$. When calculating the mean direction change over the entirety of the intervals the direction does not matter, so here absolute values were used.

3.3.8 Vertical wind speed

The output format of the anemometer gives the vertical wind speed W as a positive or negative value in the vertical direction, where positive is up and negative is down, as shown in figure 2.10 in section 2.3. The vertical wind speed that was used to plot the vertical wind speed, was modified from the $20Hz$ sampling frequency to $1Hz$ data. Every observation was then plotted against the horizontal wind speed, and against the wind direction. This representation is more accurate than when using mean values.

Chapter 4

Results and discussion

This chapter presents the measured results from the site at campus Gløshaugen in terms of wind speed and direction, the standard deviation of the 10-minute intervals, turbulence intensity as well as the wind distribution including skewness and kurtosis. The height of the anemometer was set at 3.5m above the roof during the entirety of the measuring period.

4.1 Measurements and logging

After resolving some issues with the computer logging the data, the first measurements were taken at the end of March. This data was collected with a sampling frequency of 1Hz. In the middle of April, the sampling frequency was increased to 20Hz, which is the maximum of the Gill Instruments Wind Master. The majority of the data was collected between 16.04.2021 and 20.05.2021. Unfortunately, the increased sampling frequency caused more issues with the logging due to the large files, this caused the computer to run out of memory and crash. Out of the total of 26.352.000 measurements less than 2% had to be reconstructed.

4.2 Wind direction and wind speed

The results from the 20Hz data were plotted in a wind rose as shown in figure 4.1, using the absolute horizontal wind speed. The wind rose shows the wind speeds, direction, and the distribution of wind direction. The results show that the main wind direction is from the southwest. The wind rose also shows that the wind speeds are quite low which could indicate that the anemometer is located in the recirculation zone caused by the separation on the rooftop. But when compared to the wind speeds recorded by nearby weather stations, the results are similar in terms of wind speed and direction, thus no conclusion can be drawn from these results.

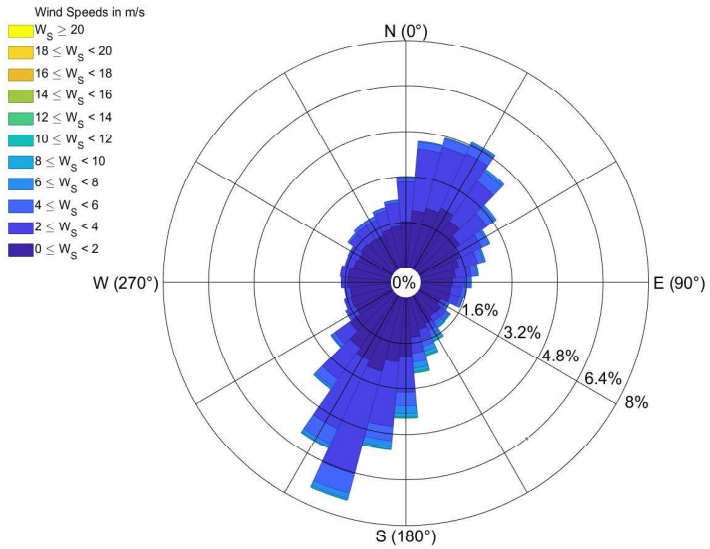

Figure 4.1: Wind rose of 366 hours with sampling frequency of 20Hz

4.3 Standard deviation

The standard deviation of the horizontal wind speed was calculated using equation 2.3. The standard deviation was calculated for every 10-minute interval as stated in the standards IEC61400-1 and IEC61400-2. Then the results were plotted against the mean wind speed in the 10-minute intervals as shown in figure 4.2. The figure also shows the comparison of the expected standard deviations defined in the IEC standards. The dots show the 10-minute observations, as well as a linear regression of the data. When comparing the two standards it's clear that the IEC61400-1 class A (high turbulence) is approximately identical to IEC61400-2 which is designed for small wind turbines. The IEC61400-1 class A+ for very high turbulence predicts a higher standard deviation than what the standard for small wind turbines does. This is expected, as the standard does not give information about the wind conditions in urban environments. The results show that the calculated standard deviation has a steeper slope than the prediction of the standards. The trend clearly shows a large deviation from the predictions of the standard. This could be the result of the majority of the data being recorded when the wind speeds were low, and more data from higher wind speeds could change the trend, causing the linear regression to be closer to the predicted values from the standards. When comparing the results from Gløshaugen to the results in *Turbulence Intensity in Complex Environments and its Influence on Small Wind Turbines (Carpman, 2011)*[15], which measures the turbulence intensity on the roof of a building in Sweden. The trends of the two sites are very similar. Both show overall low wind speeds, and an increased standard deviation compared to the IEC61400-2 standard. In the report, a slope of 0.33 was determined, which is lower than the slope parameter of 0.37 calculated in the linear regression in figure 4.2. This im-

plies that the turbulence intensity might be even higher on the roof of central building 1. More data for higher wind speeds could affect the linear regression, but due to the overall low wind speeds in the measuring interval this is unknown.

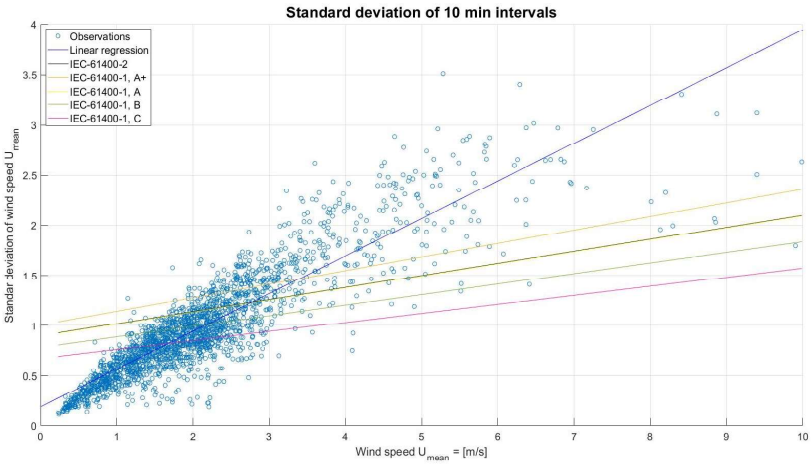

Figure 4.2: Standard deviation of wind speed, 10 minute intervals

4.4 Turbulence intensity

Figure 4.3 shows the turbulence intensity calculated according to equation 2.6 as defined in section 2.4.4. like the standard deviation, the turbulence intensity is calculated for intervals of 10 minutes. The figure shows the observations of turbulence intensity where each interval is represented by one circle, as well as the predicted turbulence intensity from IEC61400-1 and IEC61400-2. The results for the turbulence intensity directly reflect the results from the standard deviation, where the overall wind speeds are quite low. The mean turbulence intensity from all the intervals was calculated to be 49.0%. Where the turbulence intensity for wind speeds below $2.5m/s$ are lower than predicted by the standards, but after $2.5m/s$ the trend seems to be higher than the expected values. When looking at the results for turbulence intensity around $3m/s$ there are a lot of observations which are outside of the standards expected values. Increased measurements for higher wind speeds will not decrease the turbulence intensity around $3m/s$, but it might change the linear regression of the standard deviation. This has no impact on the turbulence intensity levels, except mean turbulence intensity for all intervals. But to what extent is unknown.

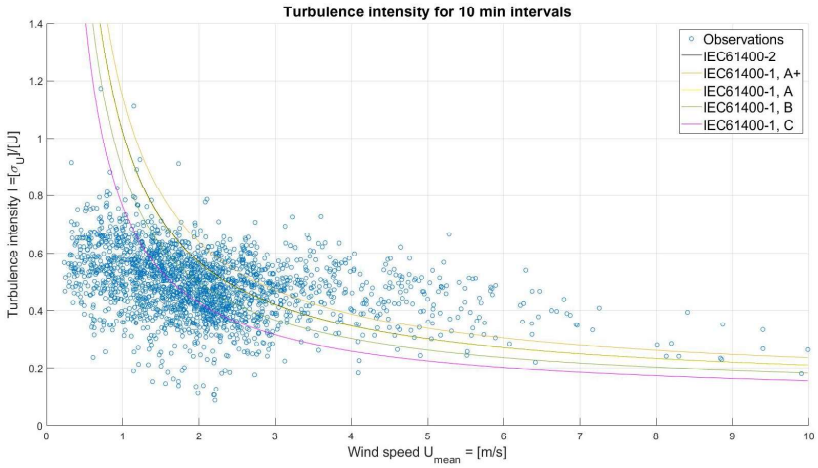

Figure 4.3: Turbulence intensity observations in 10 min intervals

These calculations do not take into account thermal stability, due to only having one measurement for temperature. When comparing the stable, near neutral and unstable results from the report *Turbulence Intensity in Complex Environments and its Influence on Small Wind Turbines (Carpman, 2011)*[15] in an urban environment, the results are so similar that they can not be distinguished from each other when plotted.

4.5 Wind direction sections

The first option as described in section 3.3.6 is to sort the data by direction first, then dividing into bins of $1m/s$, and lastly calculating the turbulence intensity in 10-minute intervals. Figure 4.4 and 4.5 shows the mean turbulence intensity and standard deviation of every 10-minute interval in each bin. Since the data is sorted before the standard deviation is calculated the data does no longer include wind speeds above the given bin, thus the data is not chronological, and since the difference in the bin now is a maximum of $0.99m/s$ the standard deviation does not give the full picture of the magnitude of the standard deviation and the turbulence intensity at the site. When comparing the results show in figure 4.4 with the results for turbulence intensity in figure 4.3 is apparent that this method underestimates the turbulence intensity drastically. Figure 4.5 shows that the trend of standard deviation is approximately the same for every bin, with the exception of the last two bins. But due to the general low wind speeds recorded, the amount of data in these bins are low, thus affecting the standard deviation and turbulence intensity. Another issue with this method is that the last interval will most likely not be exactly 12000 samples. This arises a new issue. If the data for the last interval is just shy of the 12000 samples required, the reconstruction of the data is less viable since the data is no longer chronological. And if the

reconstruction no longer is viable, what part of the data set for the given bin should be removed.

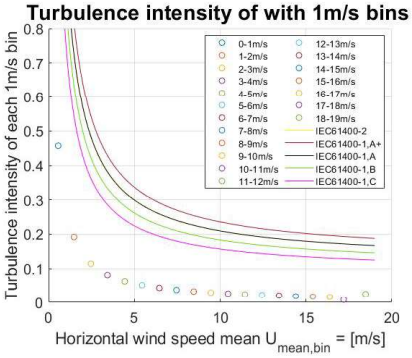

Figure 4.4: Mean TI of each 1m/s bin

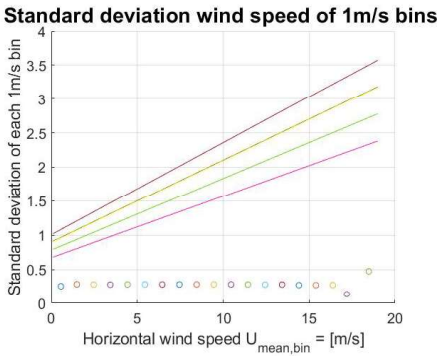

Figure 4.5: STD of each 1m/s bin

Needless to say, the first method provides a false approximation of the turbulence intensity at the site. The other alternative is to calculate the 10-minute intervals first, then divide the intervals into sections of 30° and wind speeds of $1m/s$. This method will sort the data based on the 10-minute mean direction and mean wind speed, but this alternative also arises some issues. As the intervals will contain both wind speeds outside the bins, as well as directions outside the sections. When using this method the wind data will be evaluated chronologically, and thus more true to the actual wind conditions at the site. Figure 4.6 and 4.7 shows the results for turbulence intensity and standard deviation respectably. When comparing the results from the first method in figures 4.4 and 4.5 to the results when using the second method the results correspond well with the first observations in figure 4.3, where the turbulence intensity is lower than the predicted values from the two IEC standards when the wind speeds are lower than $3m/s$. Figure 4.6 shows the mean turbulence intensity for every wind speed bin for all the sections, and show that the turbulence intensity in the bins between $4-9m/s$ exceeds the expected values for all the classes in the IEC standards. At $10m/s$ the turbulence intensity seems to be flattening out and the trend is approaching the area which is within the expected values, but due to the low amount of measurements at the higher wind speeds, there is some uncertainty associated with these results. When it comes to the standard deviation as shown in figure 4.7 the trend looks to be linear up to $7m/s$, where the standard deviation drops closer to the expected values, which also was the case for the turbulence intensity. The decrease of standard deviation in the figure is interesting and could happen due to a number of reasons. The direction when the wind speeds were higher could be from a direction with fewer disturbances, causing the changes in wind speed to be less frequent and lowering the standard deviation thus lowering the turbulence intensity.

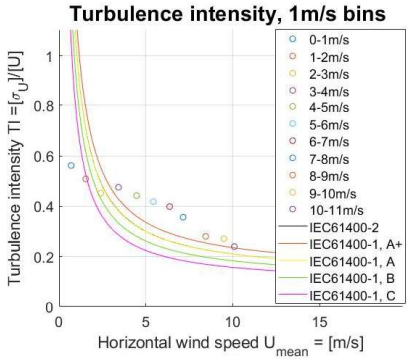

Figure 4.6: Mean TI of 10 min intervals, 1m/s bins

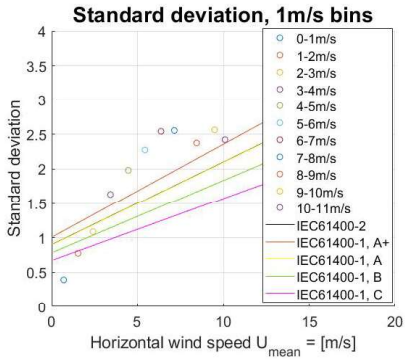

Figure 4.7: Mean STD of 10 min intervals, 1m/s bins

The main issue with this method is as described that some of the data in the 10-minute intervals will be from directions outside of the section and outside the $1m/s$ bins. This causes the evaluation for each section to be somewhat inaccurate. When comparing the two methods, the second method is the only one that gives a realistic representation of the wind conditions at the site. Figure 4.8 shows the turbulence intensity divided into sections of 30° after the 10-minute intervals were calculated. The figure is divided into four plots, where every plot has three intervals of 30° and compared to the IEC standards. The distribution of data in the plots in figures 4.8a, 4.8b, 4.8c and 4.8d are 31.4%, 16.2%, 34.0% and 18.4% respectively.

Figure 4.8a shows the results for the three sections between $0° - 89°$, which is between North and East. The section between $0° - 29°$ has an overall lower turbulence intensity until the wind speed bin $2 - 3m/s$ where it flattens out and starts to exceed the predicted values from the IEC standards. This is also the case for the section $60° - 89°$. The results between $30° - 59°$ are the only section that has all of the values for turbulence intensity within class A+. The results follow the trend from the overall turbulence intensity in figure 4.6, as they all have an increased turbulence intensity level at around $4m/s$. The wind speeds are increasing with every section, where the largest wind speed bin is in the section between $60° - 89°$, with a wind speed close to $6m/s$.

Figure 4.8b shows the results between East and South. The first section $90° - 119°$, has similar results to the last section in figure 4.8a, with almost identical turbulence intensities and wind speeds. The section between $120° - 149°$ has a higher wind speed than all the previous sections, but also an increased turbulence intensity, as it exceeds 0.5 in the wind speed bin of $4 - 5m/s$. The last section in this figure between $150° - 179°$ has very similar results to the adjacent section of $120° - 149°$. It follows the trend from the previous section, but with a slightly lower turbulence intensity. Compared to the overall results in figure 4.6, the results for all sections follow the general trend of an increased turbulence intensity level around $\sim 4m/s$, before it starts to decrease towards the predictions of the standard

again at higher wind speeds. An interesting observation is the increasing wind speeds as the wind direction approaches the South wall, this will be discussed in depth later in section 4.8.

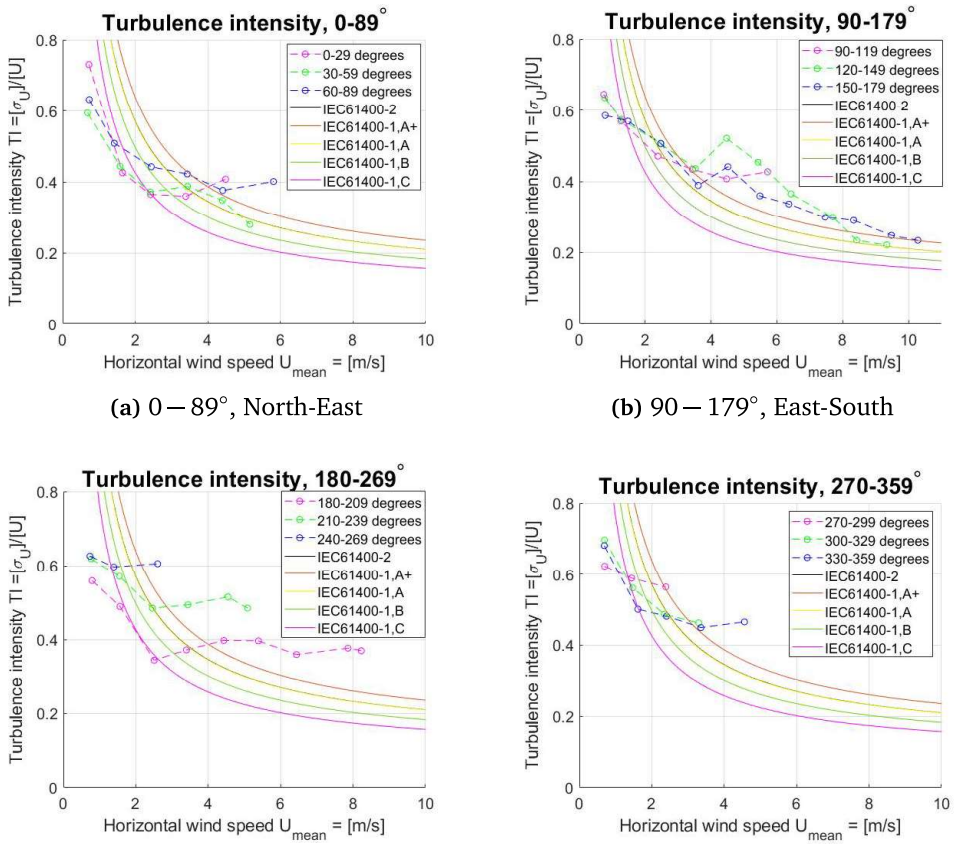

(a) $0-89^{\circ}$, North-East

(b) $90-179^{\circ}$, East-South

(c) $180-269^{\circ}$, South-West

(d) $270-359^{\circ}$, West-North

Figure 4.8: Turbulence intensity mean of 10 min intervals, divided by direction sections of 30° and 1m/s bins

Figure 4.8c shows the next sections between the South and West. The section $180^{\circ}-209^{\circ}$ has a high wind speed that correlates well with the previous section in figure 4.8b. The turbulence intensity level is slightly lower for wind speeds up to $5m/s$, but increases with higher wind speeds compared to section $150^{\circ}-179^{\circ}$. The two other sections have higher turbulence intensity and a decreasing trend in wind speed as the wind direction is moving away from the south wall. The decreasing wind speeds and increased turbulence intensity might be the results of the existing equipment mounted on the roof, shown in figure 3.4a. The obstructions on the roof is in a direct line to the anemometer between $\sim 230^{\circ} \sim 300^{\circ}$, which can be the reason why the wind speeds are lower in these sections.

Figure 4.8d shows the last sections, which have as a similar level of turbulence intensity up to $4m/s$ as the majority of section except for sections $210^{\circ}-239^{\circ}$

and $240° - 269°$. Wind speeds in the first section between $270° - 299°$ low, but increases slightly in the two sections. As discussed in figure 4.8c, the obstacles on the roof may affect the wind speeds between $\sim 230° \sim 300°$. This could be the reason why the wind speeds are so low in the first section of figure 4.8d.

One factor that needs to be considered is the influence from the central building 2, which is located around 50 meters north of the anemometer and is shown in figure 3.4a, and marked with a red star i figure 3.2. When the wind flow hits the roof of central building 2 separation is formed, which can affect the measurements at central building 1. As described in section 2.1.2, the upwind cube affects the second downwind cube. Since the height of central buildings 1 and 2 is approximately 29 meters, and the distance between them is around 56 meters this yields a distance/height factor of 1.93. As showed in figure 2.7 (b), the flow at the downwind cube is severely affected by the separation caused by the upwind cube and has a distance/height factor of 2. As the vectors also imply, the vertical wind speed should be negative.

When looking at figure 3.5, the wind directions that potentially could be affected by central building 2 is the sections between $300° \sim 340°$. The corresponding figure 4.8d, shows the wind directions that may be affected in sections $300° - 329°$ and $330° - 359°$. The two sections generally have low wind speeds, as the last section has the highest wind speed bin of $4 - 5m/s$, and the first of the two sections only having wind speed bins lower than $4m/s$. This section also has the most disturbances in terms of objects on the roof, compared to the last section. The vertical wind speed will be discussed later in section 4.8.

Another factor is that the anemometer is placed much closer to the South wall than the North wall. As described in section 2.1.2, the separation that occurs on the roof creates the phenomenons known as the acceleration zone and a recirculation zone on the roof. If the anemometer is located in the acceleration zone when the wind direction is perpendicular to the south wall, increased wind speeds should be present, as well as a positive vertical wind speed. And if the anemometer is located in the recirculation zone when the wind direction is perpendicular to the North wall, decreased wind speeds should be present.

As discussed, the wind speeds are higher in the sections $120°—210°$, which are all directions that encounter the south wall. One interesting observation is that the wind speeds in the different sections increase as the wind direction approaches the South wall at around $100°$. The highest wind speed interval is in the section $150° - 179°$. When comparing the wind direction to the figure 3.5, in section 3.2.1, the wind direction that would be perpendicular to the South wall would be $\sim 160°$. As described in section 2.1.2, the effects of the acceleration zone are at their largest when the upwind flow is perpendicular to the facade where the anemometer is located.

4.6 Wind distribution, Turbulence distribution, Skewness and Kurtosis

Figure 4.9 shows the wind speed distribution, skewness, kurtosis, and standard deviation of the 10-minute average. The distribution shows that the data set mainly have low wind speeds below $4m/s$, which is confirmed by the positive skewness and the tail of the data is to the right. The kurtosis of 8.7448 together with the skewness describes that the distribution heavily based around the low wind speeds. The assumption of a Rayleigh distributed wind speeds, stated in the IEC standards seems to correlate well with the results for wind distribution.

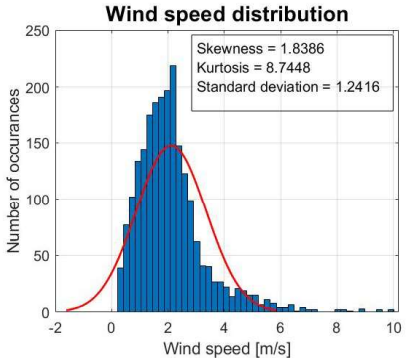

Figure 4.9: Wind speed distribution

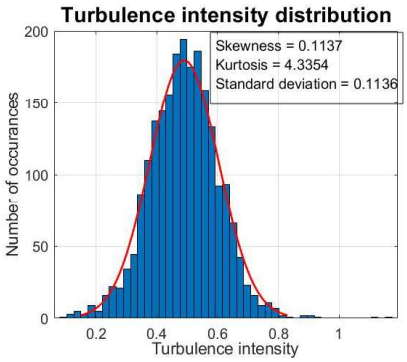

Figure 4.10: Turbulence intensity distribution

Figure 4.10 shows the distribution of turbulence intensity for the 10-minute intervals. The results show that the turbulence intensity is close to a normal distribution. The positive skewness of 0.114 shows that the distribution is almost symmetrical, but has a small tail to the right. The kurtosis of 4.34 describes that the distribution has slightly more observations of turbulence intensity around ~ 0.50 than a normal distribution, but is still close to what a normal distribution would be. The low standard deviation also describes that the turbulence intensity of the 10-minute intervals is closely spread around the mean turbulence intensity for all the intervals.

4.7 Change in wind direction

Figure 4.11 shows the distribution of wind direction change between two adjacent intervals of 1 minute, using a bin size of 4°. The directional changes were calculated as described in section 3.3.7. The low skewness of 0.0282 shows that the distribution of the directional change is close to symmetrical. The kurtosis of 6.51 describes that more values in the distribution is located around the mean than a standard deviation. Both the symmetry and that the values are heavily based around the mean are visible in figure 4.11. When comparing these results

to the results from the report *Surface Wind Direction Variability (Mahrt, 2011)*[16], which evaluated the direction change of 15 different sites with both complex and plain terrains but none in an urban environment. In these cases, the skewness is never lower than 1.3. The kurtosis from the different sites ranges from $4-45$, although this is a large range, all ranges are above a normal distribution since the kurtosis is larger than 3. When comparing the results for the directional changes, all of the cases in *(Mahrt, 2011)*[16] have a mean directional change of less than 1°. For the site at campus Gløshaugen, the mean directional change between the two adjacent intervals is 26°, which is significantly higher. When evaluating the change in direction, it is important that the data is chronological. Misleading results can accrue if the data is sorted in sections of for example 30°. If three adjacent intervals have the direction of 10°, 40° and 10° the sorting will remove the wind directions above 30°, resulting in a directional change in the section of 0°, while in reality, it is 30°.

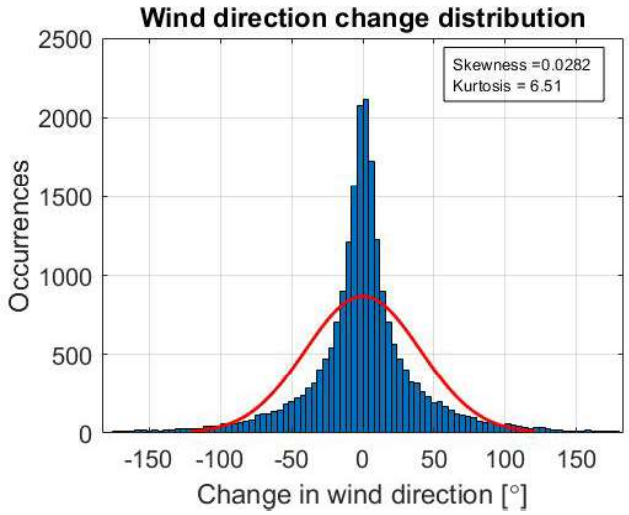

Figure 4.11: Wind direction change distribution

4.8 Vertical wind speed

The previously presented data is based on the horizontal wind speed and turbulence intensity. The vertical wind speed is often measured as a positive or negative value along the vertical plane, as described in section 3.3.8. Figure 4.12 shows the positive vertical wind speed plotted against the horizontal wind speed, after filtering the values to $1Hz$. The results show a linear regression with a slope of 0.16. In figure 4.13, the negative vertical wind speed is plotted as an absolute value for the ease of comparing the results, the linear regression with a slope of 0.010. When comparing the results to each other, it is apparent that the positive vertical wind speed has a larger overall magnitude compared to the horizontal wind

speed, as the slope is larger. Negative vertical wind speed is not present when the horizontal wind speeds exceed $\sim 14 m/s$. The distribution between negative and positive vertical wind speed is 55.8% and 44.2% respectively.

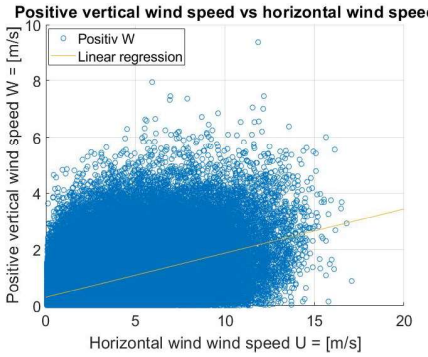

Figure 4.12: Positive vertical wind speed vs horizontal wind speed

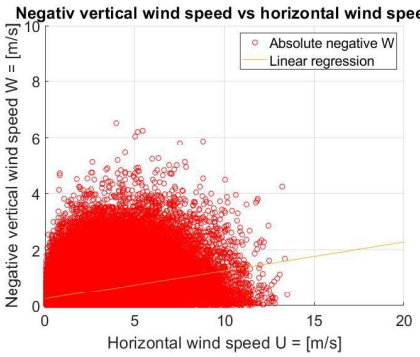

Figure 4.13: Negative vertical wind speed vs horizontal wind speed

The vertical wind speed was also plotted against the horizontal wind direction shown in figure 4.14. The figure shows that the negative wind speed has overall even wind speeds for all the wind direction, but has a slight dip around 200°. The Positive wind speed on the other hand has a large increase starting around 130° and reaches a peak at around 190° before declining down again to around 240°. Increased positive vertical wind speeds are as discussed present in the acceleration zone, and caused by the separation on the leading edge of the roof. To determine if the anemometer is located in the acceleration zone, the wind directions can be compared to figure 3.5 in section 3.2.1. As illustrated in the figure, and defined in the section the wind directions between 120° and 230° are considered to directly encounter the south wall. The increased vertical wind speeds almost line up perfectly with the expected wind directions assumed to hit the South wall, but shifted $\sim$ 10° clockwise. This could imply that the anemometer is not perfectly aligned with the north spar. The increase in positive vertical wind speed has an impact on the negative vertical wind speed, as it is reduced in the same area as the increase is present. The impact on the negative values seems to have a larger footprint, as is seems to influence the wind speeds between 100° and 270°. Outside this interval, the positive and negative wind speeds seem to have a generally similar magnitude.

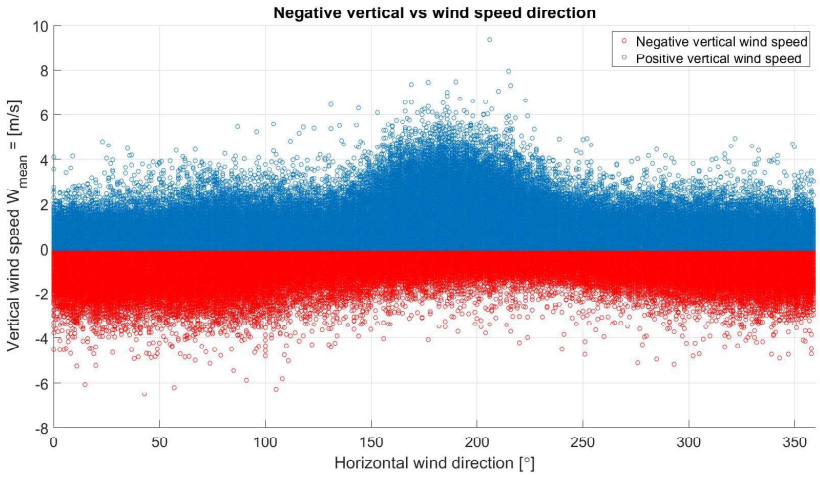

Figure 4.14: Vertical wind speed plotted against wind direction

As discussed in section 4.5, central building 2 could potentially have an effect on the wind conditions on central building 1. It this is the case, stronger negative vertical wind speed should be present between 300°—340°. When comparing the results between 300° and 340° in figure 4.14 there are no presents of increased negative wind speeds in the section. The section can also be compared to the section between 0°—40°, which shows very similar results.

Chapter 5

Conclusion

The work performed include the evaluation of standard deviation and turbulence intensity, as described in the IEC standards. As well as section analysis of the turbulence, directional change in wind direction and evaluation of the vertical wind speed.

The results regarding the standard deviation of the horizontal wind speed show that both the IEC61400-2 and IEC61400-1 (all classes) underestimate the slope of the standard deviation. The values for the standard deviation for low wind speeds below $3m/s$ lie within the range of the standard's expected values, but when exceeding $3m/s$ the majority of calculations are higher than the expected values. The normal turbulence model estimates the turbulence intensity poorly, resulting in an increased turbulence intensity for wind speeds higher than $3m/s$. The results from *(Carpman, 2011)*[15] have similarities in terms of turbulence intensity and confirms that the IEC61400-1 and IEC61400-2 standards are not suited for evaluating the wind conditions in complex urban environments.

Evaluating the wind data in sections of 30° as stated in the Measnet guidance gives a good overview of the differences in the turbulence intensity for the different sections. This is proven to give valuable information, especially in urban environments where there are more obstacles that can cause increased turbulence intensity levels.

The results regarding vertical wind speed confirm that the anemometer is located in the acceleration zone when experiencing wind directions towards the South wall. Central building 2 does not appear to have any impact on the wind conditions on central building 1, due to the uniform distribution in vertical wind speed magnitude outside the acceleration zone.

When evaluating the changes in wind direction, the results show large fluctuations with an average of 26° difference between the adjacent intervals of 1 minute. The large fluctuation in direction implies that a VAWT could be more efficient in this case, due to it not being affected by the rapid changes in wind direction compared to a HAWT.

This study has evaluated wind data recorded in a relatively short time period. Seasonal evaluation of the wind condition should be performed. More measure-

ments for different heights would also be beneficial when exploring the acceleration zone on the South wall of central building 1. Other positions on the roof could also be investigated and compared to the results presented in this report. Thermal stability could also be explored. For longer term measurements a better laptop should be considered, as the manual importing of data sets was very time consuming.

Bibliography

[1] B. H. Jorgensen. (2020). 'Iea wind tcp 2019 annual report,' [Online]. Available: https://community.ieawind.org/viewdocument/iea-wind-tcp-2019-annual-report-au?CommunityKey=3a5d79bc-c865-4e01-8ac6-19757ca91ee9&tab=librarydocuments (visited on 29/05/2021).

[2] I. E. Commission. (2021). 'What we do,' [Online]. Available: https://www.iec.ch/what-we-do (visited on 29/05/2021).

[3] R. B. Stull, *An Introduction to Boundary Layer Meteorology*. 1988.

[4] N. G. Society, 'Wind,' 2020. [Online]. Available: https://www.nationalgeographic.org/encyclopedia/wind/.

[5] N. green business ideas. (2012). 'Friction, turbulence and smart siting,' [Online]. Available: https://newgreenbusinessideas.blogspot.com/search/label/Turbulence (visited on 02/04/2021).

[6] S. Mertens, 'Wind energy in the built environment - concentrator effects of buildings,' *Wind Engineering*, vol. 30, Oct. 2006. DOI: 10.1260/030952406779502623.

[7] H. Fernando, 'Fluid dynamics of urban atmospheres in complex terrain,' *Annual Review of Fluid Mechanics*, vol. 42, no. 1, pp. 365–389, 2010. DOI: 10.1146/annurev-fluid-121108-145459. eprint: https://doi.org/10.1146/annurev-fluid-121108-145459. [Online]. Available: https://doi.org/10.1146/annurev-fluid-121108-145459.

[8] K. Sunderland, T. Woolmington, M. Conlon and J. Blackledge, 'Urban deployment of small wind turbines: Power performance and turbulence,' in *2013 48th International Universities' Power Engineering Conference (UPEC)*, 2013, pp. 1–6. DOI: 10.1109/UPEC.2013.6714858.

[9] R. Martinuzzi and B. Havel, 'Turbulent flow around two interfering surface-mounted cubic obstacles in tandem arrangement,' *Journal of Fluids Engineering-transactions of The Asme - J FLUID ENG*, vol. 122, Mar. 2000. DOI: 10.1115/1.483222.

[10] G. I. Limited. (2020). 'Windmaster 3d sonic anemometer,' [Online]. Available: http://www.gillinstruments.com/products/anemometer/windmaster.htm (visited on 04/03/2021).

[11] I. E. Commission. (2013). 'Wind turbines - part 2: Small wind turbines,' [Online]. Available: https://www.standard.no/no/Nettbutikk/produktkatalogen/Produktpresentasjon/?ProductID=674760 (visited on 14/05/2021).

[12] I. E. Commission. (2019). 'Wind energy generation systems - part 1: Design requirements,' [Online]. Available: https://www.standard.no/no/Nettbutikk/produktkatalogen/Produktpresentasjon/?ProductID=1142738 (visited on 10/05/2021).

[13] Measnet. (2016). 'Evaluation of site-specific wind conditions,' [Online]. Available: https://www.measnet.com/wp-content/uploads/2016/05/Measnet_SiteAssessment_V2.0.pdf (visited on 18/03/2021).

[14] S. N. Burkeland, 'Urban wind: Cfd analysis of gløshaugencampus based on measured data,' 2018.

[15] N. Carpman, 'Turbulence intensity in complex environments and its influence on small wind turbines,' Jan. 2011.

[16] L. Mahrt, 'Surface wind direction variability,' 2011. DOI: 10.1175/2010JAMC2560.1.

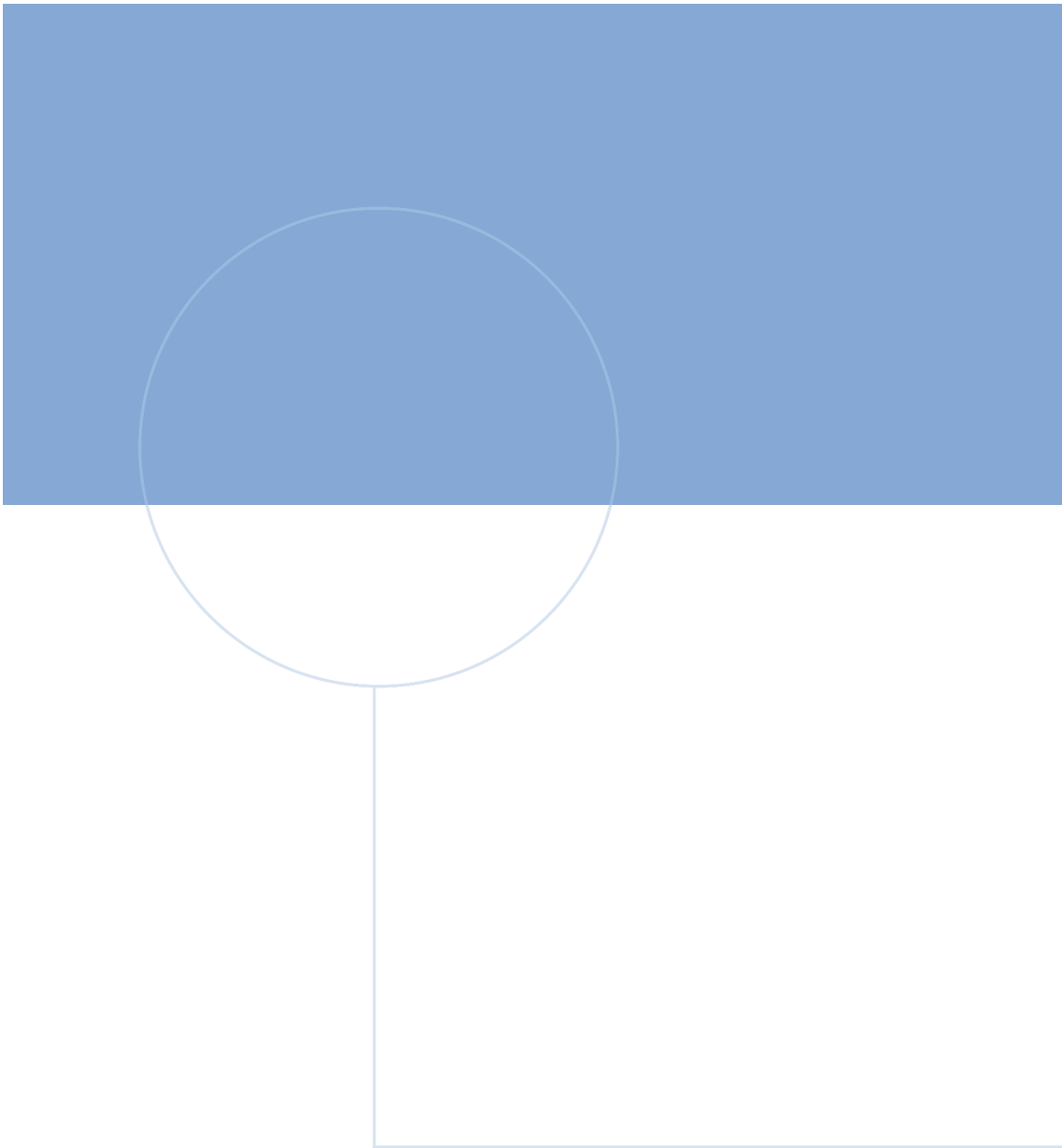

NTNU

Kunnskap for en bedre verden